

# JUST LEAF IT: ACCELERATING DIFFUSION CLASSIFIERS WITH HIERARCHICAL CLASS PRUNING

## Anonymous authors

Paper under double-blind review

## ABSTRACT

Diffusion models, best known for high-fidelity image generation, have recently been repurposed as zero-shot classifiers by applying Bayes' theorem. This approach avoids retraining but requires evaluating every possible label for each input, making inference prohibitively expensive on large label sets. We address this bottleneck with the Hierarchical Diffusion Classifier (HDC), a training-free method that exploits semantic label hierarchies to prune irrelevant branches early and refine predictions only within promising subtrees. This coarse-to-fine strategy reduces the number of expensive denoiser evaluations, yielding substantial efficiency gains. On ImageNet-1K, HDC achieves up to 60% faster inference while preserving, and in some cases even improving, accuracy (65.16% vs. 64.90%). Beyond ImageNet, we demonstrate that HDC generalizes to datasets without predefined ontologies by constructing hierarchies with large language models. Our results show that hierarchy-aware pruning provides a tunable trade-off between speed and precision, making diffusion classifiers more practical for large-scale and open-set applications.

## 1 INTRODUCTION

Diffusion models have fundamentally reshaped the landscape of image synthesis, demonstrating an unparalleled ability to model complex data distributions conditioned on inputs like class labels or text prompts (Moser et al., 2024b; Bar-Tal et al., 2023; Frolov et al., 2024; Lugmayr et al., 2022; Ho et al., 2020). This deep, generative understanding of data unlocks capabilities that extend far beyond image creation, offering a powerful new paradigm for discriminative tasks (Goodfellow et al., 2014; Rezende & Mohamed, 2015). While traditional supervised classifiers excel in static, well-labeled scenarios, they often falter in dynamic, real-world settings. Their reliance on fixed label sets necessitates extensive retraining to accommodate new classes, and they struggle with out-of-distribution or open-set data. The rich, pre-trained representations of diffusion models, however, are uniquely suited for these challenging zero-shot, open-set, and robust classification tasks (Clark & Jaini, 2023; Chen et al., 2024b; Allgeuer et al., 2024).

Capitalizing on this potential, researchers have begun repurposing pre-trained diffusion models as diffusion classifiers (Li et al., 2023; Chen et al., 2024a). The approach is elegant in its simplicity: by leveraging Bayes' theorem, a model trained to estimate  $p(\mathbf{x} | \mathbf{c})$  - the likelihood of image  $\mathbf{x}$  given class  $\mathbf{c}$  - can infer  $p(\mathbf{c} | \mathbf{x})$  - the probability of class  $\mathbf{c}$  given image  $\mathbf{x}$ . This allows for zero-shot inference without any label-specific retraining. The core mechanism involves evaluating the diffusion model's ability to reconstruct a noised input image under different class conditions, typically by estimating the noise prediction error.

Despite this compelling potential, a major computational bottleneck renders diffusion classifiers impractical for all but the smallest-scale problems (Ganguli et al., 2022; Clark & Jaini, 2023; Li et al., 2023; Moser et al., 2024a). Current methods must execute the expensive noise-prediction process for *every* potential class label for each input image, resulting in a computational cost that scales linearly with the size of the label set. While prior work has explored acceleration through weak pre-filtering of class labels (Li et al., 2023) or successive elimination (Clark & Jaini, 2023), these methods still treat the label space as flat and often evaluate a large majority of candidates.

To make diffusion classifiers more viable, we introduce the Hierarchical Diffusion Classifier (HDC), a novel, training-free approach that fundamentally restructures the classification process by exploiting semantic label hierarchies (see Figure 1). Instead of a flat, brute-force search, HDC employs a

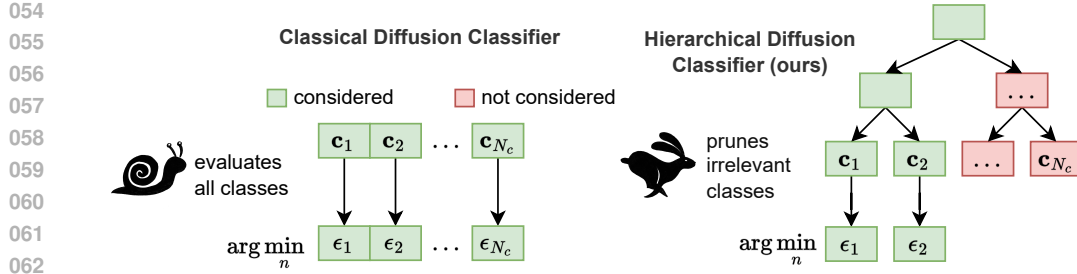


Figure 1: Comparison between the classical diffusion classifier and our proposed Hierarchical Diffusion Classifier (HDC). Whereas the classical approach evaluates all possible classes to find the correct label, which leads to unnecessary computation, HDC prunes irrelevant classes early, focusing only on the most relevant candidates. This hierarchical pruning reduces computational overhead and accelerates inference.

multi-stage, coarse-to-fine strategy. It first performs a computationally cheap evaluation at high levels of the label hierarchy (e.g., "animal" vs. "vehicle"). Based on these initial scores, HDC prunes entire branches of the label tree deemed irrelevant, drastically reducing the candidate space. It then performs the standard, more computationally intensive diffusion classification *only* on the significantly narrowed set of remaining leaf-node candidates.

Our contributions are as follows:

- We propose the Hierarchical Diffusion Classifier (HDC), a training-free method that significantly accelerates diffusion-based classification by leveraging a coarse-to-fine search on a semantic label hierarchy.
- We demonstrate that HDC reduces inference time by up to 60% on ImageNet-1K while maintaining comparable accuracy, and in some configurations, even outperforming the baseline flat classifier (65.16% vs. 64.90% average per-class accuracy).
- We introduce and evaluate both fixed and adaptive pruning strategies, providing a tunable trade-off between speed and precision that enhances the feasibility of diffusion classifiers for large-scale tasks.
- We show that our approach generalizes to datasets without pre-defined hierarchies by successfully constructing and using label trees generated by Large Language Models (LLMs).

While not intended to replace standard supervised classifiers on closed-set benchmarks, HDC represents a critical step toward making diffusion classifiers practical and scalable for the dynamic, data-scarce, and open-set scenarios where their unique generative power is most needed.

## 2 RELATED WORK

Zero-shot classification enables models to recognize categories unseen during training by leveraging shared semantics between inputs and labels. CLIP exemplifies this paradigm in vision-language modeling (Radford et al., 2021), and recent large language models extend zero-shot and few-shot classification in text domains (Achiam et al., 2023; Touvron et al., 2023; Anil et al., 2023).

Diffusion models, originally developed for image synthesis (Ho et al., 2020; Dhariwal & Nichol, 2021; Rombach et al., 2022), have been adapted for discriminative use without additional training. These *diffusion classifiers* score a label by how well a conditional diffusion model reconstructs a noised input under that label (Li et al., 2023; Clark & Jaini, 2023; Chen et al., 2024b;a). This enables flexible zero-shot and open-set classification but incurs a high cost because inference scales with the number of labels: each candidate requires a forward pass (or several) through the denoiser.

To reduce this cost, prior work has introduced flat-space candidate reduction. Li et al. (2023) pre-filter labels with a weak discriminative model, while Clark & Jaini (2023) use successive elimination in a multi-armed bandit framework. These strategies lower computation yet still treat the label set as unstructured, so most comparisons remain necessary when the label space is large.

108 Our approach departs from flat filtering by exploiting the semantic structure among labels. We  
 109 leverage dataset hierarchies (or automatically constructed label trees) to prune entire subtrees early  
 110 and refine only within relevant branches. In this sense, our method complements prior accelerations  
 111 while directly targeting scalability on large, structured label spaces.  
 112

### 113 3 PRELIMINARIES: FLAT DIFFUSION CLASSIFIER

115 We follow the formulation of Li et al. (2023) for extracting a zero-shot classifier from a conditional  
 116 diffusion model. Let  $p_\theta(\mathbf{x} \mid \mathbf{c})$  denote the likelihood of image  $\mathbf{x}$  under class prompt  $\mathbf{c}$ . By Bayes’  
 117 rule,

$$119 \quad p_\theta(\mathbf{c}_i \mid \mathbf{x}) = \frac{p(\mathbf{c}_i) p_\theta(\mathbf{x} \mid \mathbf{c}_i)}{\sum_{j=1}^{N_C} p(\mathbf{c}_j) p_\theta(\mathbf{x} \mid \mathbf{c}_j)} = \frac{p_\theta(\mathbf{x} \mid \mathbf{c}_i)}{\sum_{j=1}^{N_C} p_\theta(\mathbf{x} \mid \mathbf{c}_j)}, \quad (1)$$

121 where we assume a uniform class prior  $p(\mathbf{c}_i) = 1/N_C$ .  
 122

123 For diffusion models trained to predict noise, the evidence lower bound links the likelihood to the  
 124  $\varepsilon$ -prediction error. Writing  $\mathbf{x}_t = \sqrt{\bar{\alpha}_t} \mathbf{x} + \sqrt{1 - \bar{\alpha}_t} \varepsilon$  for the noising process with  $t \in \{1, \dots, T\}$   
 125 and  $\varepsilon \sim \mathcal{N}(0, I)$ , we obtain the posterior (up to normalization)

$$126 \quad p_\theta(\mathbf{c}_i \mid \mathbf{x}) \propto \exp \left\{ - \mathbb{E}_{t, \varepsilon} \|\varepsilon - \varepsilon_\theta(\mathbf{x}_t, \mathbf{c}_i)\|^2 \right\}, \quad (2)$$

128 where  $\varepsilon_\theta(\cdot, \mathbf{c})$  is the denoiser’s noise prediction under condition  $\mathbf{c}$ .  
 129

130 **Monte Carlo estimate.** In practice, we approximate the expectation with  $M$  samples  $(t_k, \varepsilon_k)$ :  
 131

$$132 \quad \mathbb{E}_{t, \varepsilon} \|\varepsilon - \varepsilon_\theta(\mathbf{x}_t, \mathbf{c})\|^2 \approx \frac{1}{M} \sum_{k=1}^M \left\| \varepsilon_k - \varepsilon_\theta \left( \sqrt{\bar{\alpha}_{t_k}} \mathbf{x} + \sqrt{1 - \bar{\alpha}_{t_k}} \varepsilon_k, \mathbf{c} \right) \right\|^2. \quad (3)$$

135 **Paired-difference (shared-sample) scoring.** For classification, only *relative* errors matter. Using  
 136 the same sample set  $S = \{(t_k, \varepsilon_k)\}_{k=1}^M$  across all classes increases statistical efficiency and yields  
 137 the paired-difference approximation:

$$139 \quad p_\theta(\mathbf{c}_i \mid \mathbf{x}) \approx \left[ \sum_{j=1}^{N_C} \exp \left\{ \mathbb{E}_{t, \varepsilon} (\|\varepsilon - \varepsilon_\theta(\mathbf{x}_t, \mathbf{c}_i)\|^2 - \|\varepsilon - \varepsilon_\theta(\mathbf{x}_t, \mathbf{c}_j)\|^2) \right\} \right]^{-1}. \quad (4)$$

142 This *flat diffusion classifier* thus assigns scores to all labels and normalizes across the label set,  
 143 enabling zero-shot and open-set prediction without any discriminative retraining (Li et al., 2023;  
 144 Clark & Jaini, 2023; Chen et al., 2024b;a). Its main drawback is computational: inference cost scales  
 145 linearly with  $N_C$  because each class requires evaluating the denoiser for multiple  $(t, \varepsilon)$  pairs.  
 146

### 147 4 HIERARCHICAL DIFFUSION CLASSIFIER (HDC)

149 Flat diffusion classifiers evaluate all candidate labels independently, leading to an inference cost that  
 150 scales linearly with the number of classes. To alleviate this bottleneck, we introduce the *Hierarchical*  
 151 *Diffusion Classifier* (HDC), which exploits semantic label trees to prune irrelevant branches early and  
 152 restrict expensive diffusion evaluations to a small set of promising candidates.  
 153

#### 154 4.1 TRAVERSING THE LABEL TREE

155 Let  $T_h = (N, E)$  denote a hierarchical label tree of depth  $h$ , with nodes  $N$  and edges  $E$ . Each node  
 156  $n \in N$  corresponds to a synset (or a class if  $n$  is a leaf). The root node is  $n_{\text{root}}$ , and  $\text{Children}(n)$   
 157 denotes its child nodes. Each node carries a label embedding  $\mathbf{c}_n$ . For leaves, these are class labels.  
 158

159 We begin with  $\mathcal{S}_{\text{selected}}^1 = \{n_{\text{root}}\}$ . At step  $d$ , for each selected node  $n_s \in \mathcal{S}_{\text{selected}}^d$ , we compute the  
 160  $\varepsilon$ -prediction error for its children:

$$161 \quad \epsilon_n = \mathbb{E}_{t, \varepsilon} \|\varepsilon - \varepsilon_\theta(\mathbf{x}_t, \mathbf{c}_n)\|^2, \quad n \in \text{Children}(n_s), \quad (5)$$

162 approximated via Monte Carlo sampling as in Equation 3, but with a smaller  $M$  for efficiency.  
 163

164 Based on these scores, we prune nodes by retaining only those below a threshold determined by a  
 165 pruning strategy (see Section 4.3). Formally,

$$166 \quad \mathcal{S}_{\text{selected}}^{d+1} = \{n \in \text{Children}(n_s) \mid n_s \in \mathcal{S}_{\text{selected}}^d, \epsilon_n \leq \text{threshold}(K_d)\}. \quad (6)$$

168 The process continues until depth  $h$ , where  $\mathcal{S}_{\text{selected}}^h$  contains the final leaf candidates. The final  
 169 prediction is then given by the flat diffusion classifier restricted to this pruned set:  
 170

$$171 \quad \mathbf{c}_{n_{\text{final}}}, \quad n_{\text{final}} = \arg \min_{n \in \mathcal{S}_{\text{selected}}^h} \epsilon_n. \quad (7)$$

173 By pruning aggressively, HDC reduces the number of denoiser calls from  $\mathcal{O}(N_C)$  to sublinear in  $N_C$ .  
 174 If  $b$  is the branching factor and  $K_d$  the pruning ratio at level  $d$ , the cost scales as  
 175

$$176 \quad \mathcal{O}(N_C^{1+\log_b K} M C_\varepsilon), \quad 1 + \log_b K < 1, \quad (8)$$

178 where  $C_\varepsilon$  is the cost of one  $\varepsilon_\theta$  evaluation. In practice, speed-up is roughly  $1/K$  compared to flat  
 179 diffusion classification.  
 180

## 181 4.2 TREE SETUP

183 HDC requires a label hierarchy but is not tied to a specific source. For ImageNet-1K, we use the  
 184 WordNet ontology (Deng et al., 2009), pruning overly vague nodes (*e.g.*, ‘entity’ or ‘artifact’) and  
 185 collapsing redundant subtrees, yielding a depth-7 hierarchy. For datasets without native ontologies  
 186 (*e.g.*, CIFAR-100, Food101, Oxford Pets), we construct trees using large language models to generate  
 187 semantic groupings. This demonstrates HDC’s flexibility: it leverages existing taxonomies when  
 188 available and synthesizes plausible ones otherwise.  
 189

## 190 4.3 PRUNING STRATEGIES

191 We implement two pruning strategies:

- 193 • **Fixed Pruning.** At each level, retain the top- $K_d$  fraction of nodes with lowest error scores.
- 194 • **Dynamic Pruning.** At each level, retain nodes within  $2\sigma_d$  of the minimum error, *i.e.*,

$$197 \quad \mathcal{S}_{\text{selected}}^{d+1} = \{n \in \text{Children}(n_s) \mid n_s \in \mathcal{S}_{\text{selected}}^d, \epsilon_n \leq \epsilon_{\min}^d + 2\sigma_d\}, \quad (9)$$

198 where  $\epsilon_{\min}^d$  and  $\sigma_d$  denote the minimum and standard deviation of error scores at depth  $d$ .  
 199

200 Fixed pruning provides explicit control over the speed–accuracy trade-off, while dynamic pruning  
 201 adapts automatically to the score distribution. Both lead to substantial runtime reductions, as shown  
 202 in our experiments section.  
 203

## 204 4.4 DYNAMIC CLASS MODIFICATION

206 Unlike discriminative classifiers, HDC naturally supports dynamic class modifications. Removing  
 207 a class corresponds to pruning its leaf; adding a class amounts to inserting a new leaf under an  
 208 appropriate parent (either predefined or selected greedily). This property makes HDC particularly  
 209 suited to open-set and evolving label spaces.  
 210

## 211 5 EXPERIMENTS

213 This section presents our experimental setup and results, evaluating different aspects of HDC: pruning  
 214 strategies, prompt engineering, SD variations, and an overall evaluation of per-class accuracy on  
 215 various datasets. Our code will be published upon acceptance.

216  
 217 Table 1: **ImageNet-1K comparison** of overall and per-class classification accuracy and inference  
 218 time between the classical diffusion classifier (Li et al., 2023) and our proposed HDC (fixed and  
 219 adaptive pruning) using Stable Diffusion 2.0. HDC achieves significant inference time reduction  
 220 (up to 60%) while maintaining or improving accuracy. The best results are marked in bold, the  
 221 second-best underlined.

Method	Pruning	Avg. Accuracy [%]		Time [s]	Speed-Up [%]
		Overall	Per-Class		
Flat Diffusion Classifier (Li et al., 2023)	—	64.70	64.90	1600	—
HDC (ours)	Fixed	<b>64.90</b>	<b>65.16</b>	980	<u>38.75</u>
HDC (ours)	Adaptive	63.20	63.33	<b>650</b>	<b>59.38</b>

## 229 5.1 SETUP

231 HDC is based on the efficient framework established by Li et al. (2023), with added modifications  
 232 tailored for hierarchical processing and pruning of candidate classes, further customized for diffusion  
 233 classification on Stable Diffusion (SD) (Rombach et al., 2022). Yet, our method is adaptable, allowing  
 234 seamless integration with different diffusion models and possible fine-tuning to support various  
 235 hierarchical pruning strategies. To demonstrate this, we accommodate the SD versions 1.4, 2.0, and  
 236 2.1. For fixed pruning, we set  $K_d = 0.5$  for all possible  $d$ -values. All evaluations were performed at  
 237  $512 \times 512$ , the resolution under which all versions of SD were originally trained. Also following Li  
 238 et al. (2023), we used the  $l_2$  norm to compute the  $\varepsilon_t$ -predictions and sampled the timesteps uniformly  
 239 from  $[1, 1000]$ .

240 For Imagenet-1K (Deng et al., 2009), the class labels are converted to the form “a photo of a *<class*  
 241 *label>*” using the template from the original work (Li et al., 2023). Inspired by Radford et al. (2021),  
 242 we also experiment with prompt templates “A bad photo of a *<class label>*”, “A low-resolution  
 243 photo of a *<class label>*” and “itap of a *<class label>*”. For CIFAR-100 (Krizhevsky, 2009), we  
 244 use “a blurry photo of *<class label>*”. Finally, for the Food101 (Bossard et al., 2014) and Pets  
 245 (Parkhi et al., 2012) datasets, we use the template “a photo of a *<class label>*, a type of food/pet.”

## 246 5.2 MAIN RESULTS

247 Table 1 highlights the results of our HDC with both pruning strategies (fixed and adaptive) compared  
 248 to the classical, flat diffusion classifier (Li et al., 2023) on ImageNet-1K.

249 **Overall.** As observed, both pruning strategies show significant improvements in runtime compared  
 250 to classical diffusion classifiers, and each is suited to different prioritizations of speed versus accu-  
 251 racy. Fixed pruning yields the best trade-off results on ImageNet-1K, achieving significant runtime  
 252 reductions (up to 980 seconds) with a top-1 accuracy boost of 0.20 percentage points. By employing  
 253 adaptive pruning (selecting candidates based on two standard deviations from the lowest error), we  
 254 reduce the inference time even further to 650 seconds, though at the cost of a slight accuracy drop  
 255 (*i.e.*, 1.50 percentage points). The adaptive strategy demonstrates that faster inference can be achieved  
 256 with a small compromise in precision.

257 **Per-Class.** The baseline diffusion classifier achieves an accuracy of 64.90% with an inference time  
 258 of 1600 seconds, providing a reference for both speed and precision. Using fixed pruning in HDC  
 259 demonstrates new state-of-the-art accuracy for diffusion classifiers with 65.16%, while reducing  
 260 the inference time by nearly 40% to 980 seconds. This indicates that HDC can not only improve  
 261 classification performance but also leads to a considerable reduction in computation. Reducing  
 262 processing time while maintaining similar accuracy makes fixed pruning a balanced choice for  
 263 high-accuracy applications where inference speed is a priority. Similarly, HDC with adaptive pruning  
 264 leverages dynamic pruning to further accelerate inference. While it records a slight drop in accuracy  
 265 to 63.33%, adaptive pruning reduces inference time to 650 seconds - approximately 60% faster than  
 266 the baseline. This strategy demonstrates the potential of HDC for use cases requiring faster response  
 267 times, with only a marginal trade-off in classification performance.

270  
 271  
 272  
 273  
 274  
 275  
**Table 2: CIFAR-100 with an LLM-generated label tree (SD 2.0).** We report class-wise Top-  
 276 accuracy and runtime per class for the flat diffusion classifier versus HDC with *fixed* pruning  
 277 ( $K_d \in \{0.75, 0.5, 0.4\}$ ) and *adaptive* pruning (retain nodes with  $\epsilon \leq \epsilon_{\min}^d + 2\sigma_d$ ). HDC consistently  
 278 reduces inference cost while preserving or improving accuracy; *e.g.*, fixed pruning with  $K_d=0.4$   
 279 improves accuracy by +3.3 pp and cuts runtime by  $\approx 34\%$  relative to the flat baseline. Best results  
 280 are in **bold**, second-best are underlined.  
 281

	Flat Diff. Classifier (Li et al., 2023)	Fixed Pruning			Adaptive Pruning
		$K_d = 0.75$	$K_d = 0.5$	$K_d = 0.4$	$\leq \epsilon_{\min}^d + 2\sigma_d$
Class-Acc [%]	68.93	56.79	60.57	<b>72.23</b>	65.12
Runtime [s/class]	1000	<u>275</u>	<u>550</u>	660	740
Speed-Up [%]	-	<b>72.50</b>	<u>45.00</u>	34.00	<u>26.00</u>

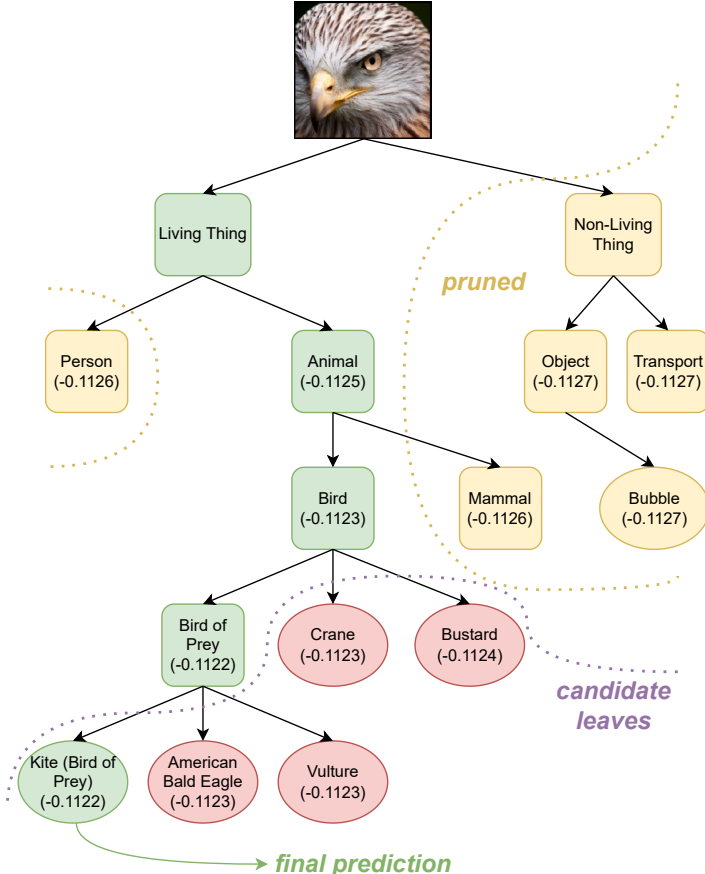
282  
 283  
 284 **Example.** Figure 2 illustrates how HDC progressively prunes the label tree.  
 285 At each stage, error scores guide the elimination of unlikely branches, leaving only  
 286 a small set of relevant leaf nodes. The final prediction is then obtained by applying  
 287 the flat diffusion classifier on this reduced set, demonstrating how HDC shifts expen-  
 288 sive computation to only the most promising candidates.  
 289  
 290

291 **Confusion.** The confusion matrix in Figure 3 shows within the ‘‘Animal’’ subtree.  
 292 Misclassifications predominantly occur among biologically similar classes (*e.g.*,  
 293 salamanders vs. lizards, or lizards vs. snakes), indicating that the model’s errors  
 294 are structured and semantically meaningful.  
 295  
 296

297 **Summary.** Our results  
 298 highlight that HDC enables  
 299 a tunable trade-off between  
 300 inference speed and accu-  
 301 racy. Fixed pruning delivers  
 302 the best balance of efficiency  
 303 and precision, making it  
 304 suitable for high-stakes  
 305 classification, while adaptive  
 306 pruning achieves the fastest  
 307 runtimes with only minor  
 308 accuracy loss.  
 309  
 310

### 311 5.3 LLM-GENERATED LABEL-TREES AND OTHER DATASETS

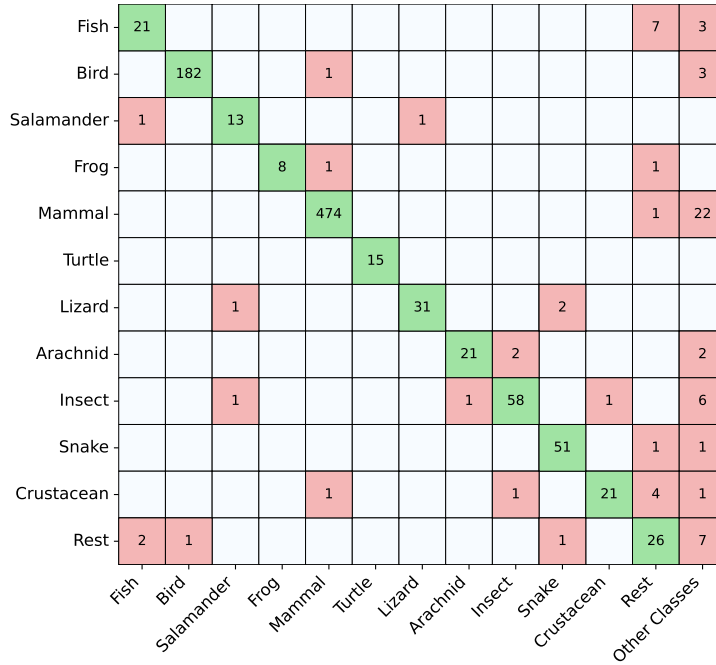
312 Our method also demonstrates notable results on CIFAR-100 when employing a LLM-generated  
 313 label hierarchy, substantially outperforming the standard flat diffusion classifier (see Table 2).  
 314  
 315



316 **Figure 2: Illustration of HDC on a single image.** At each stage,  
 317 nodes with high error scores are pruned, leaving only relevant branches  
 318 of the label tree. Here, pruning progressively narrows the candidates  
 319 to semantically related classes (*e.g.*, American Bald Eagle, Vulture),  
 320 before selecting the correct leaf node *Kite (Bird of Prey)* as the final  
 321 prediction. This example completes in 1102 seconds, demonstrating  
 322 how HDC focuses computation on a compact set of plausible labels.  
 323

324  
 325 Table 3: Performance of HDC with fixed and adaptive pruning on **Pets** and **Food101** using LLM-  
 326 generated label trees. Across both datasets, HDC accelerates inference while maintaining or improv-  
 327 ing accuracy: *e.g.*, +2.1 pp on Pets and +2.8 pp on Food101 compared to the flat diffusion classifier.  
 328 Best results are shown in **bold**.

	Pets			Food101		
	Top1 [%]	Top5 [%]	Time [s]	Top1 [%]	Top5 [%]	Time [s]
Flat Diffusion Classifier (Li et al., 2023)	85.25	99.19	40.55	72.40	<b>92.00</b>	79.22
HDC fixed (ours)	86.53	98.69	40.00	<b>75.15</b>	88.95	66.60
HDC adaptive (ours)	<b>87.39</b>	<b>99.39</b>	<b>40.00</b>	67.00	81.15	<b>52.60</b>



357 Figure 3: **Confusion matrix on ImageNet-1K (“Animal” subtree).** Results shown for HDC with  
 358 fixed pruning. The y-axis denotes ground-truth classes and the x-axis predicted labels (including  
 359 “other classes” outside the subtree). Most confusions occur between semantically related species (*e.g.*,  
 360 salamander-lizard, lizard-snake), reflecting meaningful structure in the model’s errors.

363 Moreover, we show the influence of the pruning ratio  $K_d$  for our fixed pruning strategy critically  
 364 dictates the balance between classification accuracy and inference speed. For instance, decreasing  $K_d$   
 365 from 0.75 to 0.5, and further to 0.4, shows a clear trend: accuracy improves from 56.79% to 60.57%  
 366 and then to a peak of 72.23%, while runtime correspondingly increases from 275s to 550s and 660s.

367 Finally, the performance advantages of HDC generalize effectively to other datasets, such as Pets and  
 368 Food101, as detailed in Table 3. For instance, on the Pets dataset, HDC adaptive improved Top-1  
 369 accuracy by +2.14pp (to 87.39%) with a negligible change in runtime (40s vs. 40.55s). On the Food  
 370 dataset, HDC fixed simultaneously increased Top-1 accuracy by +2.75 percentage points (to 75.15%)  
 371 and accelerated inference by a significant 16% (66.6s vs. 79.22s). Even greater speed-ups were  
 372 observed with HDC adaptive on Food (52.6s, a 33.6% reduction), albeit with a trade-off in accuracy  
 373 for that specific configuration.

#### 375 5.4 STABLE DIFFUSION VERSIONS

376 We evaluated the HDC using different SD versions to assess its flexibility and performance across  
 377 generative backbones, as summarized in Table 4. The results reveal that SD 2.0 provides the best

378  
 379 Table 4: Performance comparison of the **HDC with different diffusion models** using fixed and  
 380 adaptive pruning for **ImageNet-1K**. Top-1 accuracy and inference time (in seconds) are reported for  
 381 each SD version, highlighting SD 2.0 as achieving the highest accuracy, while adaptive pruning in  
 382 SD 1.4 yields the fastest inference time.

SD Version	Fixed Pruning				Adaptive Pruning			
	Top 1 [%] (class-wise)	Top 1 [%] (overall)	Time [s]	Speed-Up [%]	Top 1 [%] (class-wise)	Top 1 [%] (overall)	Time [s]	Speed-Up [%]
SD 1.4	52.71	52.60	1000	37.50	54.77	54.80	710	55.63
SD 2.0	<b>65.16</b>	<b>64.90</b>	980	38.75	<b>63.33</b>	<b>63.20</b>	980	38.75
SD 2.1	61.15	61.00	<b>950</b>	<b>40.63</b>	60.91	60.70	720	55.00

383  
 384  
 385 Table 5: Evaluation **across different prompt types** for HDC using fixed and adaptive pruning on  
 386 **ImageNet-1K**. The standard prompt, “A photo of a *<class label>*”, consistently yields the highest  
 387 Top-1, Top-3, and Top-5 accuracy. Alternative prompts, such as “A bad photo of a *<class label>*”  
 388 and “A low-resolution photo of a *<class label>*”, result in slight decreases in accuracy, showing that  
 389 prompt variations can impact model performance.

Pruning	Prompt-Type	Top 1 [%]	Top 3 [%]	Top 5 [%]
fixed	“A photo of a <i>&lt;class label&gt;</i> ”	<b>64.90</b>	<b>80.20</b>	<b>85.30</b>
	“A bad photo of a <i>&lt;class label&gt;</i> ”	59.90	79.60	84.90
	“itap of a <i>&lt;class label&gt;</i> ”	61.37	81.33	86.30
	“A low-resolution photo of a <i>&lt;class label&gt;</i> ”	57.50	76.46	80.94
adaptive	“A photo of a <i>&lt;class label&gt;</i> ”	<b>63.20</b>	<b>82.30</b>	<b>86.30</b>
	“A bad photo of a <i>&lt;class label&gt;</i> ”	62.30	80.10	85.90
	“itap of a <i>&lt;class label&gt;</i> ”	57.80	78.20	82.30
	“A low-resolution photo of a <i>&lt;class label&gt;</i> ”	57.50	76.46	80.94

405  
 406 trade-off between accuracy and inference time. Specifically, when using fixed pruning, SD 2.0  
 407 achieved the highest Top-1 accuracy at 64.14% with an inference time of 980 seconds. In contrast,  
 408 SD 1.4 demonstrates the fastest inference time of 710 seconds when paired with adaptive pruning,  
 409 albeit with a significant top-1 class-accuracy reduction to 54.77%.

## 411 5.5 PROMPT ENGINEERING

412 Inspired by Radford et al. (2021), we also evaluated different prompt templates to assess their impact  
 413 on accuracy and inference time, as shown in Table 5. The default prompt, “a photo of a *<class  
 414 label>*”, consistently achieved the best performance, suggesting that a straightforward prompt yields  
 415 robust results across classes. Other templates, such as “a bad photo of a *<class label>*” and “a  
 416 low-resolution photo of a *<class label>*”, resulted in a slight drop in accuracy without significantly  
 417 affecting inference time.

418 The rationale for testing alternative prompts stems from a hypothesis that prompts hinting at lower-  
 419 quality images might help the classifier generalize better to real-world cases with variable quality,  
 420 capturing diverse visual characteristics. For instance, using terms like “bad” or “low-resolution” was  
 421 expected to enhance robustness to noisy or degraded inputs.

422 Interestingly, however, the results show that the simpler, unmodified prompt performs best, indicating  
 423 that the hierarchical model likely benefits from a more neutral prompt format when dealing with  
 424 high-quality image data like ImageNet-1K. Nevertheless, these prompt variations may still hold  
 425 potential for datasets with inherently low-resolution or distorted images, where quality-based prompts  
 426 could help the classifier learn more generalized features.

427 We also observed a significant disparity in inference times across specific classes, such as “snail” (221  
 428 seconds) versus “keyboard space bar” (1400 seconds). This difference likely reflects the complexity  
 429 of visual features within each category: classes with intricate or ambiguous features may require  
 430 longer processing times due to the hierarchical classification structure.

432 

## 6 LIMITATIONS & FUTURE WORK

433  
434 Although HDC delivers substantial speed-ups and competitive accuracy, including in robust and  
435 zero-shot open-set settings with dynamic class modifications, several limitations open avenues for  
436 future research.437 Most importantly, the efficiency gains hinge on the depth and balance of the label hierarchy. Datasets  
438 with shallow trees or weak semantic groupings may see limited acceleration. This motivates the  
439 development of more sophisticated, data-driven hierarchies that can adapt to the structure of each  
440 dataset. Likewise, our method has yet to be tested on domains with highly complex or overlapping  
441 categories, such as medical imaging or fine-grained visual recognition. These scenarios present  
442 opportunities to extend HDC with adaptive thresholds, weighted traversal paths, or hybrid pruning  
443 strategies that emphasize fine-grained discriminative cues.444 Looking forward, we see three especially promising directions: (i) automated hierarchy construction  
445 using LLMs or representation learning, (ii) tighter integration with multimodal diffusion models to  
446 support cross-domain classification, and (iii) dynamic, task-aware pruning strategies that adapt in real  
447 time. Together, these directions point to a broader research agenda: turning diffusion classifiers into  
448 scalable, flexible, and general-purpose tools for large-scale recognition.449  
450 

## 7 CONCLUSION

451  
452 We presented the Hierarchical Diffusion Classifier (HDC), a training-free framework that makes  
453 diffusion-based classification practical at scale. By replacing flat evaluation with a coarse-to-fine  
454 search over semantic label hierarchies, HDC prunes entire branches early and focuses computation  
455 only on the most promising candidates. This simple but powerful idea yields up to a 60% reduction  
456 in inference time while matching, or even surpassing, the accuracy of flat diffusion classifiers.457 Beyond efficiency, HDC introduces a new design principle for diffusion classifiers: exploiting  
458 structure in the label space. Our experiments show that both fixed and adaptive pruning strategies  
459 deliver flexible control over the speed–accuracy trade-off, enabling deployment in settings ranging  
460 from high-accuracy benchmarks to real-time applications. Crucially, HDC generalizes across datasets  
461 with and without predefined hierarchies, demonstrating that scalable diffusion classification is  
462 achievable even in dynamic, open-set environments.463 In short, HDC expands the role of diffusion models from generative foundations to competitive,  
464 large-scale classifiers. We believe this hierarchical perspective opens the door to a new class of  
465 diffusion-based methods that are not only expressive but also efficient, adaptive, and ready for  
466 real-world recognition tasks.467  
468 

## REFERENCES

469  
470 Josh Achiam, Steven Adler, Sandhini Agarwal, Lama Ahmad, Ilge Akkaya, Florencia Leoni Aleman,  
471 Diogo Almeida, Janko Altenschmidt, Sam Altman, Shyamal Anadkat, et al. Gpt-4 technical report.  
472 *arXiv preprint arXiv:2303.08774*, 2023.  
473 Philipp Allgeuer, Kyra Ahrens, and Stefan Wermter. Unconstrained open vocabulary image classification:  
474 Zero-shot transfer from text to image via clip inversion. *arXiv preprint arXiv:2407.11211*,  
475 2024.  
476 Rohan Anil, Andrew M. Dai, Orhan Firat, Melvin Johnson, Dmitry Lepikhin, . . . , and Yonghui Wu.  
477 Palm 2 technical report. *arXiv preprint arXiv:2305.10403*, May 2023.  
478 Omer Bar-Tal, Lior Yariv, Yaron Lipman, and Tali Dekel. Multidiffusion: Fusing diffusion paths for  
479 controlled image generation. 2023.  
480 Lukas Bossard, Matthieu Guillaumin, and Luc Van Gool. Food-101–mining discriminative compo-  
481 nents with random forests. In *ECCV*, pp. 446–461. Springer, 2014.  
482 Huanran Chen, Yinpeng Dong, Shitong Shao, Zhongkai Hao, Xiao Yang, Hang Su, and Jun Zhu.  
483 Your diffusion model is secretly a certifiably robust classifier. *arXiv preprint arXiv:2402.02316*,  
484 2024a.

486 Huanran Chen, Yinpeng Dong, Shitong Shao, Hao Zhongkai, Xiao Yang, Hang Su, and Jun Zhu.  
 487 Diffusion models are certifiably robust classifiers. *NeurIPS*, 37:50062–50097, 2024b.  
 488

489 Kevin Clark and Priyank Jaini. Text-to-image diffusion models are zero-shot classifiers, 2023. URL  
 490 <https://arxiv.org/abs/2303.15233>.

491 Jia Deng, Wei Dong, Richard Socher, Li-Jia Li, Kai Li, and Li Fei-Fei. Imagenet: A large-scale  
 492 hierarchical image database. In *CVPR*, pp. 248–255. Ieee, 2009.

493

494 Prafulla Dhariwal and Alexander Nichol. Diffusion models beat gans on image synthesis. *NeurIPS*,  
 495 34:8780–8794, 2021.

496 Stanislav Frolov, Brian B Moser, and Andreas Dengel. Spotdiffusion: A fast approach for seamless  
 497 panorama generation over time. *arXiv preprint arXiv:2407.15507*, 2024.

498

499 Deep Ganguli, Danny Hernandez, Liane Lovitt, Amanda Askell, Yuntao Bai, Anna Chen, Tom  
 500 Conerly, Nova Dassarma, Dawn Drain, Nelson Elhage, et al. Predictability and surprise in large  
 501 generative models. In *2022 ACM Conference on Fairness, Accountability, and Transparency*, 2022.

502 Ian Goodfellow, Jean Pouget-Abadie, Mehdi Mirza, Bing Xu, David Warde-Farley, Sherjil Ozair,  
 503 Aaron Courville, and Yoshua Bengio. Generative adversarial networks. In *NeurIPS*, 2014.

504

505 Jonathan Ho, Ajay Jain, and Pieter Abbeel. Denoising diffusion probabilistic models. *NeurIPS*, 33:  
 506 6840–6851, 2020.

507

508 Alex Krizhevsky. Learning multiple layers of features from tiny images. Technical re-  
 509 port, University of Toronto, 2009. URL <https://www.cs.toronto.edu/~kriz/learning-features-2009-TR.pdf>.

510

511 Alexander C Li, Mihir Prabhudesai, Shivam Duggal, Ellis Brown, and Deepak Pathak. Your diffusion  
 512 model is secretly a zero-shot classifier. In *ICCV*, pp. 2206–2217, 2023.

513

514 Andreas Lugmayr, Martin Danelljan, Andres Romero, Fisher Yu, Radu Timofte, and Luc Van Gool.  
 515 Repaint: Inpainting using denoising diffusion probabilistic models. In *CVPR*, 2022.

516

517 Brian B Moser, Federico Raue, Sebastian Palacio, Stanislav Frolov, and Andreas Dengel. Latent  
 518 dataset distillation with diffusion models. *arXiv preprint arXiv:2403.03881*, 2024a.

519

520 Brian B Moser, Arundhati S Shanbhag, Federico Raue, Stanislav Frolov, Sebastian Palacio, and  
 521 Andreas Dengel. Diffusion models, image super-resolution and everything: A survey. *arXiv  
 522 preprint arXiv:2401.00736*, 2024b.

523

524 Omkar M Parkhi, Andrea Vedaldi, Andrew Zisserman, and CV Jawahar. Cats and dogs. In *CVPR*, pp.  
 525 3498–3505. IEEE, 2012.

526

527 Alec Radford, Jong Wook Kim, Chris Hallacy, Aditya Ramesh, Gabriel Goh, Sandhini Agarwal,  
 528 Girish Sastry, Amanda Askell, Pamela Mishkin, Jack Clark, Gretchen Krueger, and Ilya Sutskever.  
 529 Learning transferable visual models from natural language supervision, 2021. URL <https://arxiv.org/abs/2103.00020>.

530

531 Danilo Rezende and Shakir Mohamed. Variational inference with normalizing flows. pp. 1530–1538.  
 532 PMLR, 2015.

533

534 Robin Rombach, Andreas Blattmann, Dominik Lorenz, Patrick Esser, and Björn Ommer. High-  
 535 resolution image synthesis with latent diffusion models. In *CVPR*, pp. 10684–10695, 2022.

536

537 Hugo Touvron, Louis Martin, Zev Stone, Samson Albert, Abdelrahman Almahairi, Marwan Elmadaidy,  
 538 Charlotte de Masson d’Autume, Vasudev Kosaraju, Sharan Bhosale, John Schulman Inc, Julien  
 539 Lespiau, Luke Zettlemoyer, and Armand Joulin. LLaMA: Open and efficient foundation language  
 540 models. In *Proceedings of the 40th International Conference on Machine Learning (ICML)*, pp.  
 541 130:1–130:20, 2023.